Membrane Capacitance Changes Associated with Particle Uptake during Phagocytosis in Macrophages

Kathleen O. Holevinsky and Deborah J. Nelson
Department of Pharmacological and Physiological Sciences, The University of Chicago, Chicago, Illinois 60637 USA

ABSTRACT We report the use of capacitance measurements to monitor particle uptake after cellular exposure to phagocytic stimuli. In these studies, human monocyte-derived macrophages (HMDMs) and cells from the murine macrophage-like cell line J774.1 were exposed to immune complexes or sized latex particles (0.8 or 3.2 μm in diameter). An average decrease in cell capacitance of 8 pF was seen after exposure of the cells to immune complexes. Cells in which particle uptake was inhibited by cytochalasin B treatment before exposure to immune complexes showed an average increase of 0.5 pF. The decrease in membrane capacitance after exposure of cells to particulate stimuli was absent with the soluble stimulus, platelet-activating factor, further confirming that decreases in membrane capacitance were due to particle uptake. Exposure of cells to sized latex particles resulted in a graded, stepwise decrease in membrane capacitance. The average step size for 0.8-μm particles was 250 fF, and the average step change for the larger 3.2-μm particles was 480 fF, as calculated from Gaussian fits to the step size amplitude histograms. The predicted step size for the individual particles based upon the minimum amount of membrane required to enclose a particle and a specific capacitance of 10 fF/μm^2 was 20 and 320 fF, respectively. The step size for the smaller particles deviates significantly from the predicted size distribution, indicating either a possible lower limit to the size of the phagocytic vacuole or multiple particles taken up within a single phagosome. Dynamic interaction between phagocytosis and exocytosis was observed in a number of cells as a biphasic response consisting of an initial rapid increase in capacitance, consistent with cellular exocytosis, followed by stepwise decreases in capacitance.

INTRODUCTION

Phagocytosis of particulate stimuli by monocytes results in the release of preformed granule contents into either the phagosome, a process termed degranulation, or discharge of granular contents outside of the cell, termed exocytosis or secretion (Henson et al., 1988). We have previously shown that human monocyte-derived macrophages (HMDMs) phagocytize immune complexes under voltage-clamp conditions after whole-cell formation (Holevinsky and Nelson, 1995). In those experiments, the release of free radicals within the phagocytic vacuole, which is the end point of particle uptake, was visualized through the use of fluorophores covalently linked to the immune complex. The time course for particle binding and uptake, however, could not be resolved. Because the cellular response to particle uptake is complex, we now report the use of time-resolved measurements of membrane capacitance to determine the sequence of individual events that occur.

The measurement of membrane capacitance has become an important technique for studying exocytosis, endocytosis, and stimulus-secretion coupling mechanisms in a variety of cells (Neher and Marty, 1982; Zimmerberg et al., 1987; Breckenridge and Almers, 1987a,b; Neher, 1988; Schweizer et al., 1989; Thomas et al., 1990; Horrigan and Bookman, 1994; Lindau and Fernandez, 1986; Parsons et al., 1994; Artalejo et al., 1994). Membrane capacitance is proportional to cell surface area. Therefore, changes in membrane capacitance provide a direct and quantitative record of the time course of cytoplasmic granule insertion into the plasma membrane during exocytosis. Alternatively, particle uptake or plasma membrane retrieval during membrane recycling can also be monitored directly by capacitance measurements. Although the technique has been used to study membrane retrieval after episodes of secretion (Thomas et al., 1990; Parsons et al., 1994), there have been no studies to date using the technique to follow particle uptake during phagocytosis.

The phagocytic event is initiated by the binding of a microorganism to specific surface receptors on phagocytes, e.g., monocytes, macrophages, and neutrophils. Receptors involved in this interaction include those recognizing the C3b/C3b′ fragments of complement (Wright and Silverstein, 1982) and those that interact with the Fc domain of immunoglobulin G (Odin et al., 1990; Odin et al., 1991; Suzuki, 1991). The receptor-ligand interaction triggers a series of cellular and molecular events involving phosphoinositol turnover. Inositol phosphate and diacylglycerol formation lead to a rise in intracellular calcium (Ca_i), calcium-induced actin polymerization, and the formation and internalization of a phagocytic vacuole. The contents of cytoplasmic granules are secreted, and oxygen metabolites are generated through the activation of membrane-bound NADPH oxidase.

Macrophages are capable of ingesting particles varying in size, from bacteria to latex particles 1–14 μm in diameter, as well as a variety of mammalian and avian erythrocytes (Griffin et al., 1975; Voronov et al., 1998). Earlier light

Received for publication 10 July 1997 and in final form 4 August 1998.

Address reprint requests to Dr. Deborah J Nelson, The University of Chicago, Department of Pharmacological and Physiological Sciences, MC 2030, 5841 S. Maryland Ave., Chicago, IL 60637. Tel.: 773-702-0126; Fax: 773-702-4066; E-mail: dnelson@drugs.bsd.uchicago.edu.

0006-3495/98/11/2577/10 $2.00

microscopic studies carried out on peritoneal macrophages and a monocytic tumor cell line, J774.1, illustrated the striking phagocytic capacity of the inflammatory cells (Snyderman et al., 1977). Snyderman and colleagues demonstrated that single cells were capable of internalizing more than 200 latex particles per cell after a 45-min incubation period (see Fig. 1 (Snyderman et al., 1977)). In studies by Griffin, macrophages ingested an average of 7–16 immunoglobulin G (IgG)-coated erythrocytes per cell (Griffin et al., 1975). J774.1 cells have been shown to internalize particles through attachment to C3 and Fc receptors in a manner resembling that of activated macrophages (Kaplan and Morland, 1978). The phagocytic activity of J774.1 cells is approximately two- to fourfold greater than that of unstimulated macrophages (Snyderman et al., 1977). We compared the phagocytosis of immune complexes, which were able to bind and cross-link Fc receptors, to that of nondegradable latex beads. The average decrease in membrane capacitance appeared to be critically dependent upon both the size and composition of the particle to which the cell was exposed. Changes in membrane capacitance in response to immune complexes occurred rapidly, with step size rarely resolvable. The cellular response to latex particles occurred more slowly and was associated with smaller, more discrete changes in capacitance.

The phagocytic event was frequently coupled to exocytosis in the stimulated phagocytes. Capacitance increases of 3.0–8.4 pF, approximately three times the initial capacitance of the cell, have been shown in human neutrophils when secretory granules fuse with the plasma membrane (Nuesse and Lindau, 1988). In capacitance experiments carried out on cultured neutrophils, Nuesse and Lindau calculated that ~5900 secretory granules fused with the membrane during neutrophil degranulation (Nuesse and Lindau, 1988). In similar experiments, Fernandez calculated that a mast cell ~11 μm in diameter would contain 1020 secretory granules ~0.77 μm in diameter and reported an increase in mast cell capacitance from 5.2 pF at rest to ~13 pF after degranulation (Fernandez et al., 1984).

Macrophages and J774.1 cells, like neutrophils and mast cells, release lysosomal enzymes outside the cells in varying amounts under both unstimulated and endotoxin-stimulated conditions (Morland and Kaplan, 1978). Voronov et al. showed that macrophages release increased amounts of in-

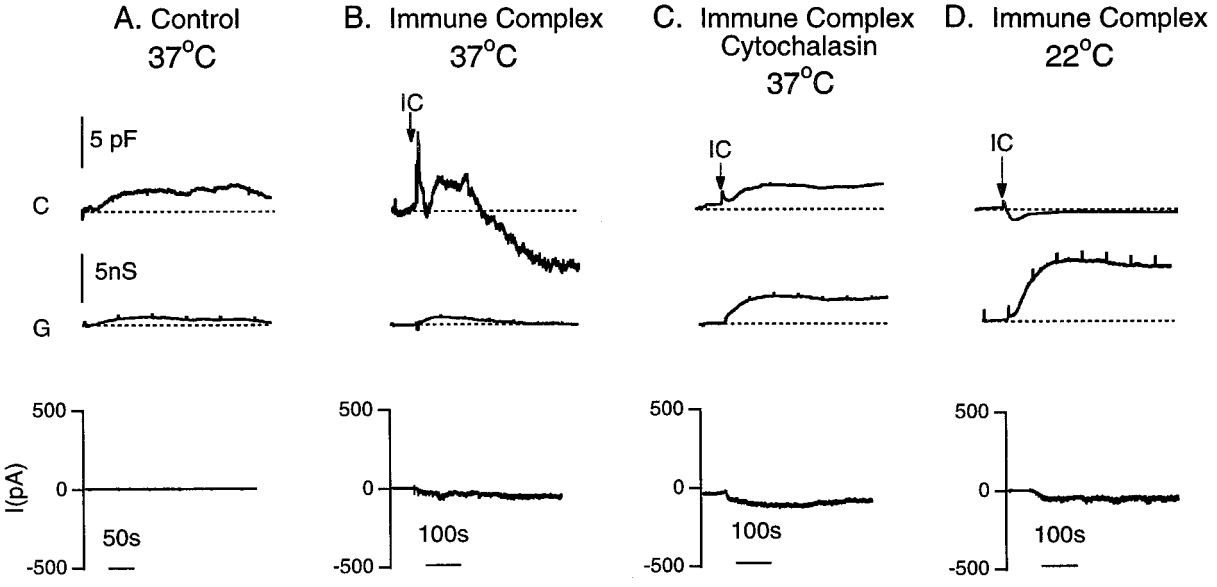

FIGURE 1 Changes in membrane capacitance in four different J774.1 cells after immune complex stimulation. Immune complex uptake at 37°C was compared to that obtained under conditions in which phagocytosis is inhibited, e.g., in the presence of actin cytoskeleton disruption with cytochalasin B and low temperature. After whole cell formation, cells were allowed to reach a steady state for 10 min before stimulus additions. Therefore, time 0 in all recordings is following a 10-min period of whole cell recording and equilibration at the indicated temperature. Cells were incubated for 2 h in 200 ng/ml pertussis toxin before stimulation with immune complex (IC), as indicated by the arrow in each recording, to prevent NADPH oxidase activation and free radical conductance activation. Capacitance measurements were made as described in the Materials and Methods section in a bath K^+-free solution containing 1 mM La^{3+}, 100 mM 4,4′-diisothiocyanatostilben-2,2′-disulfonic acid, and 5 mM tetraethylammonium to block current activation. A K^+-free bath solution was used to prevent activation of the inwardly rectifying K^+ conductance (IRK1), which is expressed at high levels in both the HMDMs and J774.1 cells, from which it was first cloned (Kubo et al., 1993). The pipette solution contained (in mM) 140 KCl, 1 EGTA, 0.2 $CaCl_2$, 2 $MgCl_2$, and 10 HEPES buffered to pH 7.2. Each panel consists of capacitance (*upper*), conductance (*middle*), and whole-cell current trace (*lower*) at −40 mV. (*A*) Control recording of a 24 pF cell, at 37°C, in which no immune complex was added. (*B*) Recording of a 16-pF cell at 37°C, after exposure of a cell to immune complex (IC), as indicated by the arrow. (*C*) Recording of a 16-pF cell after incubation of a cell with 5 μM cytochalasin B to inhibit the phagocytic response; the temperature was maintained at 37°C. Immune complex was added to the bath solution at the arrow. (*D*) Recording made in a 25-pF cell at room temperature (22°) in which lowering experimental temperature inhibited the phagocytic response. Note that resistance dithers seen as periodic deflections on the conductance traces do not project onto the capacitance trace, thereby indicating proper phase angle determination allowing separation of the series conductance and membrane capacitance, respectively (see Materials and Methods).

flammatory cytokines and lysosomal enzymes in response to stimulation with polyethylene particles (Voronov et al., 1998). In the experiments that we describe in our studies, absolute separation of endocytosis from exocytosis was difficult in the case of particulate stimuli, as has been observed for chromaffin cells (Smith and Betz, 1996). We therefore undertook studies that allowed for comparison of capacitance changes after exposure of the cells to soluble versus particulate stimuli. We used platelet-activating factor as the soluble stimulus, which we have shown to elicit a rapid increase in Ca_i and transmembrane current in cultured HMDMs (Katnik and Nelson, 1993). We compared the response to the inflammatory cytokine to that observed after exposure to the particulate stimulus heat-aggregated IgG that binds to and cross-links macrophage surface Fc receptors (Nelson et al., 1985). Both stimuli elicited a rapid increase in membrane capacitance, presumably due to exocytois. A secondary decrease in capacitance, sometimes to well below prestimulus levels, was observed after stimulation of cells with polymeric IgG complexes. This secondary decrease in capacitance was absent in cells stimulated with the soluble stimulus platelet activating factor (PAF) and was therefore attributed to particle uptake during phagosome formation.

MATERIALS AND METHODS

Cell culture

Human monocyte-derived macrophages (HMDMs) isolated from peripheral blood were cultured in Teflon vials for up to 2 weeks as previously described (Nelson et al., 1990). J774.1 cells were obtained from ATCC and were cultured in RPMI 1640 supplemented with 5% fetal bovine serum and 1% penicillin/streptomycin. Cells were plated on 35-mm plastic tissue culture dishes for up to a week before the electrophysiological experiments.

Electrophysiology

Whole-cell recordings from both HMDMs and J774.1 cells were obtained by the techniques of Hamill et al. (1981). The capacitance measuring system used to monitor particle uptake was based on the phase tracking technique developed by Fernandez et al. (Fidler and Fernandez, 1989; Fidler-Lim et al., 1990; Joshi and Fernandez, 1988). Capacitance data, including measurement of cell size, were generated on a Macintosh Centris 650 running IGOR Pro (WaveMetrics) in combination with the Pulse Control XOPs (external operations) written by Dr. Richard Bookman at the University of Miami as previously described (Horrigan and Bookman, 1994). Data were acquired using an ITC-16 analog-to-digital converter interface from Instrutech Corp. To measure changes in cell capacitance, a 500-Hz, 30-mV RMS sine wave was added to the stimulus input of the patch-clamp amplifier (EPC-7; List Electronics, Darmstadt, Germany). The resulting current was analyzed at two orthogonal phase angles from the stimulus, ϕ and $\phi - 90$, using a software-based phase-sensitive detector (PSD) (Joshi and Fernandez, 1988) with a temporal resolution of 16 ms per point. The phase detector was aligned so that one output reflected the real part of the changes in cell admittance (Re [ΔY]), and the second output reflected the imaginary part (Im [ΔY]). These outputs are proportional (not equal) to the series conductance and membrane capacitance, respectively. These approximations are valid when the cell membrane resistance is very large, in the absence of ion channel activity, and when the cell can be modeled as a simple, single time constant electrical equivalent circuit. The phase tracking technique allowed the determination of the correct phase angle for the PSD through periodic adjustments (Fidler and Fernandez, 1989). Conductance and capacitance values were continuously generated by the software. The DC current was also recorded throughout the determination of membrane capacitance and series conductance. A 500-kΩ resistor in series with the cell input impedance and ground was switched in and out during sinusoidal stimulation, and the deflections produced in the conductance served as a 500-kΩ calibration for series resistance. Correct alignment of the PSD was achieved when these series resistance changes did not project into the capacitance plot. The whole-cell capacitance was compensated completely with the slow capacitance compensation before exposure of the cells to the phagocytic stimulus. A calibration signal for the capacitance trace was obtained by unbalancing the C-slow potentiometer of the compensation circuitry of the patch-clamp amplifier by 1 pF.

Solutions

Experiments were carried out using a pipette solution that contained (in mM) 140 KCl, 1 EGTA, 0.2 $CaCl_2$, 2 $MgCl_2$, 10 HEPES buffered to pH 7.2. The bath solution contained 130 NaCl, 1 $CaCl_2$, and 10 HEPES, pH 7.4. Solution osmolarities were monitored with a vapor pressure osmometer (model 5500; Wesco, Logan, UT) and measured to be 290 mOs. In some experiments, cells were incubated with pertussis toxin (200 ng/ml) at 37°C in a humidified, 5% CO_2 environment for 2 h before the electrophysiological investigations.

Materials

Immune complexes were obtained as Fc-Oxyburst from Molecular Probes (Eugene, OR). These bovine serum albumin (BSA)–anti-BSA immunoglobulin immune complexes were coupled to the reduced fluorochrome 2′,7′-dichlorodihydrofluorescein (DCFH) and have been used in previously published studies from our laboratory to monitor superoxide release in phagocytes after particle uptake (Holevinsky and Nelson, 1995).

Cytochalasin B, pertussis toxin, and the latex particles were all obtained from Sigma (St. Louis, MO). Diphenylene iodonium (DPI) was obtained from Toronto Research Chemicals (Ontario, Canada). Human IgG was obtained from Accurate Chemical (Westbury, NY). Heat-aggregated IgG was prepared as previously described (Nelson et al., 1985).

Data analysis

Summary data are expressed as means ± standard error of the mean, with the number of experiments in parentheses unless otherwise indicated.

RESULTS

Changes in membrane capacitance were measured after exposure of HMDMs and cells from the murine macrophage cell line, J774.1, to a number of phagocytic stimuli. Experiments were carried out on individual cells, using the whole-cell configuration of the patch-clamp technique, under conditions designed to inhibit ion channel activity. Bath solutions were K^+-free to eliminate inward K^+ currents. Inhibitors of NADPH oxidase activity were used to minimize free-radical-induced current activation after phagosome formation (see Holevinsky and Nelson, 1995). Voltage-clamped cells were held at the appropriate experimental temperature for 10 min to allow for cellular stabilization before the addition of a stimulus. Immune complexes and sized latex particles were used as phagocytic stimuli.

Immune complex uptake

Fig. 1 compares changes in membrane capacitance in a voltage-clamped cell under control conditions with three other J774.1 cells after immune complex exposure. All cells were pretreated with pertussis toxin (200 ng/ml) 2 h before whole-cell voltage clamping to inhibit NADPH oxidase activation and, therefore, large changes in conductance that accompany free radical release during the phagocytic response (Holevinsky and Nelson, 1995). The DC component of the membrane current (Fig. 1, *lower panel*) and the series conductance changes (Fig. 1, *middle panel*) are shown in addition to the capacitance changes (Fig. 1, *upper panel*) to demonstrate that changes in capacitance during phagocytosis occur independently, without changes in conductance and whole-cell current, and are not an artifact of those changes. We often observed spontaneous exocytosis, indicated by a stepwise increase in capacitance, immediately after the establishment of the whole-cell clamp configuration, when cells were maintained at 37°C. This response was allowed to proceed to a steady state before capacitance recording. Fig. 1 *A* is representative of a cell under control conditions, at 37°C in the absence of a phagocytic stimulus. In cells exposed to immune complex, a significant decrease in capacitance, which was not necessarily stepwise, was observed, as in Fig. 1 *B*. Under conditions in which phagocytosis was inhibited, large decreases in capacitance after exposure to immune complex were not observed. Phagocytosis was inhibited either by pretreating cells with cytochalasin B (5 μM) for 10 min before electrophysiological recording (Fig. 1 *C*), or by maintaining the cells at room temperature during treatment with immune complex (Fig. 1 *D*). Previous reports have shown that immune complex uptake is inhibited by >80% at 20°C as compared with uptake determined at 37°C (Odin et al., 1991). Cytochalasin B has been shown not only to inhibit particle uptake (Ryan et al., 1990), but also to inhibit free radical release after exposure of cells to phagocytic stimuli (Holevinsky and Nelson, 1995), presumably because of an inhibition of particle uptake. The slow increase in capacitance that was periodically seen under conditions in which phagocytosis was inhibited, in the presence or absence of immune complex, could indicate an imbalance in the ongoing membrane fusion and retrieval process that favors vesicle fusion under the conditions of whole-cell voltage clamp. Alternatively, it could indicate a secretory response to pipette attachment, which is normally offset with particle uptake in cells undergoing phagocytosis. And finally, it could represent an increase in exocytotic fusion events due to a change in intracellular hydrostatic pressure via the patch pipette, as has been observed recently for mast cells (Solsona et al., 1998). These results are summarized in Table 1.

Latex particle uptake

Membrane capacitance changes were monitored in J774.1 cells, as well as HMDMs, after exposure to sized latex beads as the phagocytic stimulus. The cellular response to latex particles was less reactive and, therefore, did not require pretreatment with pertussis toxin to inhibit conductance activation due to free radical release. After some delay, exposure of the voltage-clamped cells to 0.8 μm beads resulted in the staircase-like decrease in capacitance as a result of retrieval of phagocytic vacuoles, as can be seen in Fig. 2. The average decrease in capacitance for nine cells exposed to 0.8-μm beads was 3.2 $\pm$ 1.3 pF. When cells were exposed to larger particles, 3.2 μm in diameter, step decreases in capacitance were, on average, larger in amplitude, as seen in the records in Fig. 3, and were often followed by a rapid but smaller increase in capacitance (see Fig. 3 *A*). Exposure of cells to the larger particles often elicited a sustained secretory response, as seen in the four cells in Fig. 3, upon which the large endocytotic events were

TABLE 1 Summary of changes in membrane capacitance evoked in single voltage-clamped HMDMs and J774.1 cells after stimulation with immune complex

Stimulus	*N*	Temp. (°C)	Initial capacitance (in pF) mean $\pm$ SD	Capacitance change (in pF) mean $\pm$ SD	*p* value*
Control	8	37	38.5 $\pm$ 31.5	8.0 $\pm$ 12	0.005
Immune complex	8	37	29.9 $\pm$ 16.8	$-$7.2 $\pm$ 4.9	—
Immune complex	5	22	47.0 $\pm$ 17.3	$-$1.0 $\pm$ 3.6	0.003
Immune complex and cytochalasin B	7	37	32.6 $\pm$ 16.7	0.5 $\pm$ 3.1	0.025

Capacitance was determined as described in Materials and Methods. After whole-cell formation, cells were allowed to reach a steady state for 10 min before stimulus additions. Cells maintained at 37°C were incubated with pertussis toxin (200 ng/ml) 2 h before electrophysiological investigations. In some experiments, cells were incubated with cytochalasin B (5 μM) ~10 min before electrophysiological experiments. Capacitance change was measured as the difference between cell size at the addition of immune complex and the final cell size ~5 min later. A total of 28 cells were examined in the experiments summarized here, of which 18 were HMDMs with an average initial membrane capacitance of 44.6 $\pm$ 23.0 pF and 10 were J774.1 cells with an average initial membrane capacitance of 20.7 $\pm$ 4.7 pF (mean $\pm$ SD). The numbers of the different cell types under each experimental condition were as follows: five HMDMs and three J774 cells under control conditions at 37°C, five HMDMs and three J774 cells at 37°C after immune complex stimulation, four HMDMs and one J774.1 cell at room temperature after immune complex stimulation, and four HMDMs and three J774.1 cells treated with cytochalasin B after immune complex stimulation.

*The significance of the difference between means was determined using a two-tailed Student's *t* test. Levels of significance were determined between changes in capacitance after immune complex stimulation and all other conditions. Note that the decrease in the level of significance between the means at 37°C and 22°C in the presence of immune complex reflects the fact that phagocytosis was not completely inhibited at 22°C.

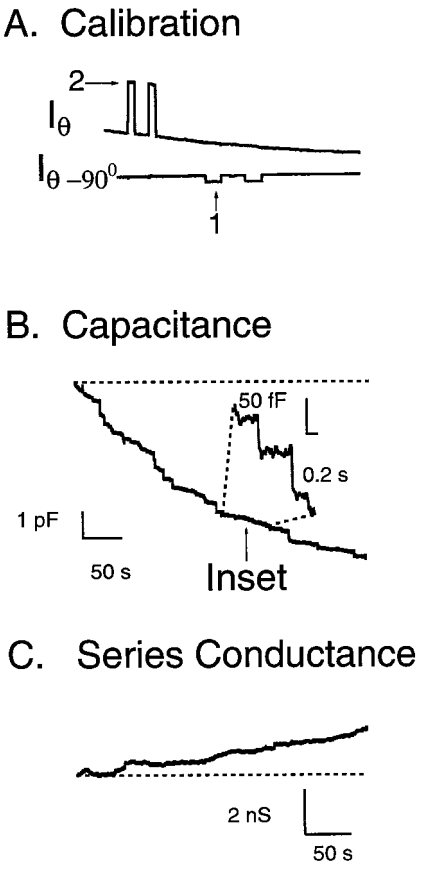

FIGURE 2 Stepwise changes in the capacitance of an HMDM (70 pF) undergoing endocytosis of 0.8-μm latex beads at 37°C, at a holding potential of −60 mV. (*A*) The individual traces show components of the current measured at each of the phase angles, θ (conductance) and $\theta - 90°$ (capacitance). Arrow 1 marks the 1-pF calibration signal for the capacitance trace obtained by unbalancing the C-slow potentiometer of the compensation circuitry of the patch-clamp amplifier, and arrow 2 represents 500-kΩ calibration for series resistance. (*B*) Recording of the cell membrane capacitance as a function of time in the HMDMs after exposure to 0.8-μm latex particles. Steps represent the phagocytosis of either one bead or a number of beads. Membrane capacitance decreases from 71 to 65 pF. Note that the scale bars are enlarged for the inset. The predicted decrease in capacitance for a single bead is 20 fF. (*C*) Change in membrane conductance during the endocytic process shown in *B*. The pipette solution contained (in mM) 140 KCl, 1 EGTA, 0.2 $CaCl_2$, 2 $MgCl_2$, 10 HEPES buffered to pH 7.2. The bath solution contained 130 NaCl, 1 $CaCl_2$, and 10 HEPES, pH 7.4.

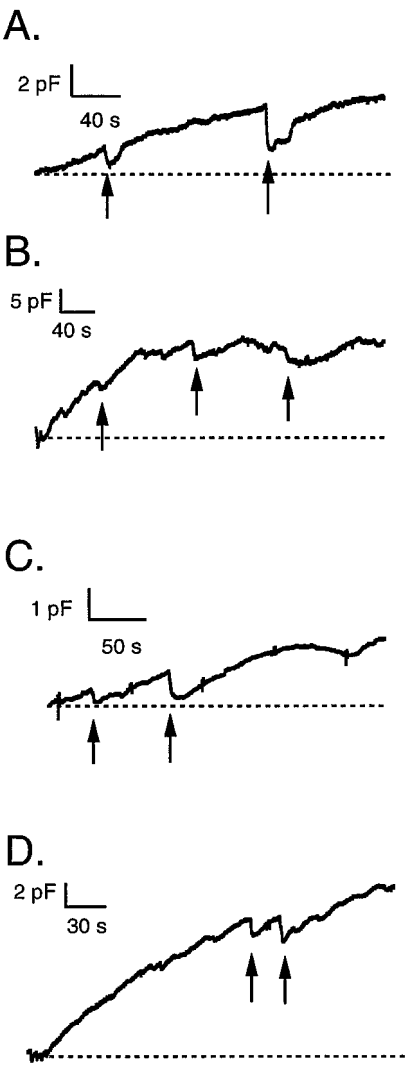

FIGURE 3 Stepwise changes in the capacitance of four cells undergoing endocytosis of 3.2-μm latex beads. Traces were taken from records acquired 2–5 min after addition of 3.2-μm latex beads to the voltage-clamped cells. Experiments were conducted at 37°C at a holding potential of −60 mV. Sharp decreases in capacitance presumed to be due to particle uptake are indicated by the arrows. Exposure of cells to the larger latex particles elicited an increase in capacitance or exocytotic response, upon which the larger decreases were infrequently observed. (*A*) Recording from a HMDM with an initial capacitance of 53 pF. (*B*) J774.1 cell with an initial capacitance of 59 pF. (*C*) J774.1 cell with an initial capacitance of 29 pF. (*D*) J774.1 cell with an initial capacitance of 30 pF. Note that calibration bars vary for each record.

infrequently observed. Histograms of step changes in membrane capacitance after exposure to the sized particles are given in Fig. 4. Gaussian fits to the amplitude histograms yielded a mean step size of 250 fF for the smaller particles and 480 fF for the larger particles. Calculations using 10 fF/μm^2 as the specific membrane capacitance predicted a step size of 20 and 320 fF for the 0.8-μm and 3.2-μm particles, respectively, based upon the minimum amount of membrane required to enclose an individual particle.

Exocytosis

The incorporation of vesicle membranes into the plasma membrane can be directly assayed as an increase in membrane capacitance or area. When cells were maintained at 37°C, membrane capacitance frequently increased slowly, either under control conditions (as seen in Fig. 1 *A*) or under conditions in which the phagocytic response was inhibited (as in Fig. 1 *C*). Increases in membrane capacitance were observed after exposure and uptake of latex particles, as seen in Fig. 5. Of note in Fig. 5 is the large of degree of heterogeneity in exocytotic step size in a single cell as well as from cell to cell. The observed heterogeneity 1) may be due to a heterogeneity in the distribution of secretory granule size or 2) may represent heterogeneity in the granule

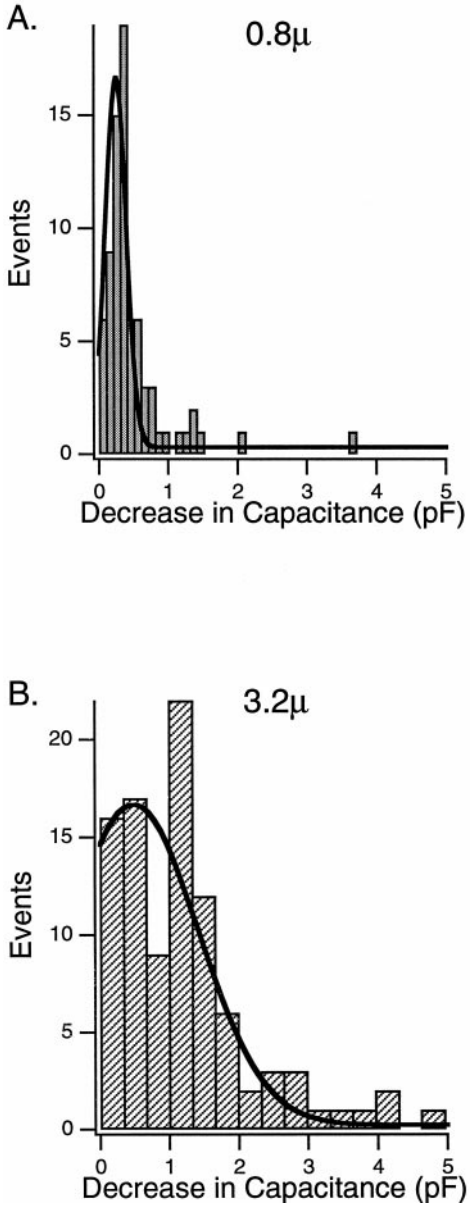

FIGURE 4 Size distribution of step decreases in capacitance after exposure of J774.1 cells and HMDM cells to latex particles at 37°C. Measurements were collected after exposure of cells to latex particles in experiments similar to those of Fig. 2. (*A*) Step size distribution histogram for 12 cells exposed to 0.8-μm latex particles. Of the 12 cells, four were HMDMs and eight were J774.1. (*B*) Step size distribution histogram for nine cells (three HMDMs and six J774.1) stimulated with 3.2-μm latex particles. Each cell was exposed to only one particle size. The theoretically predicted step size for a 0.8-μm particle is 20 fF, and that for a 3.2-μm particle is 320 fF. A conversion factor of 10 fF/μm^2 for the cell membrane was used to estimate the cell capacitance from the surface area. Steps were scored by visual inspection of the capacitance traces and thresholded at 50 fF. The average step size for the smaller particles as determined by Gaussian fits to the distribution was 250 fF for the smaller particles (number of events = 77) and 480 fF for the larger particles (number of events = 101). The size distribution for the latex particles was 0.8 $\pm$ 0.04 μm and 3.2 $\pm$ 0.2 μm (mean $\pm$ SD). The initial membrane capacitance values were 56.6 $\pm$ 20.8 pF for the HMDMs used in these studies and 24.5 $\pm$ 12.6 pF for the J774.1 cells (mean $\pm$ SD).

fusion/secretion cycle. Some cells demonstrated "capacitance flicker" as in Fig. 5 *A*. Similar capacitance "flicker" associated with the secretory response has been described for the degranulating mast cell (Fernandez et al., 1984).

Capacitance changes after stimulation with soluble versus particulate stimuli

Cellular responses to particulate and soluble stimuli were compared in J774.1 cells, as seen in Fig. 6. Our goal for the experiments depicted in Fig. 6 was to compare the response to stimuli that both elicited a respiratory burst and a secretory response but differed only in their ability to elicit phagosome formation. If decreases in membrane capacitance were due to membrane retrieval or rapid endocytosis plus phagosome formation after a secretory response, then one should be able to observe the retrieval phase in isolation with a soluble stimulus applied under conditions in which phagocytosis was inhibited, i.e., low temperature. Membrane retrieval after a maximum secretory response has been observed previously at room temperature in chromaffin cells (Artalejo et al., 1995, 1996). When J774.1 cells were stimulated with 100 μg/ml heat-aggregated IgG (HAIGG), capacitance changes were biphasic in nature, consisting of a rapid secretory phase that rose to a peak within 36.4 $\pm$ 13.8 s (n = 6). All cells stimulated with HAIGG underwent a secretory phase. The exocytotic burst was followed by a rapid reuptake phase as seen in Fig. 6 *A*. The decrease in membrane capacitance took place over a time course of 285 $\pm$ 35 s (n = 6), with step decreases in capacitance often discernible (see *inset* to Fig. 6 *A*). The decrease in membrane capacitance after cellular degranulation could represent retrieval of excess membrane, as has been observed for mast cells (Fernandez et al., 1984), adrenal chromaffin cells (Artalejo et al., 1995), and synaptic terminals (von Gersdorff and Matthews, 1994), phagosome formation, or some combination of both endocytotic events. To separate the process of membrane retrieval from receptor-mediated phagocytosis, the cellular response to HAIGG, a particulate stimulus, was compared with that after stimulation of the cells with the soluble inflammatory cytokine, platelet-activating factor (PAF). The cellular capacitance changes in response to PAF (20 ng/ml) can be seen in Fig. 6 *B*. Unlike the biphasic response observed for HAIGG, the response to PAF, consisting only of a secretory phase, reached a maximum after 213 $\pm$ 60 s (n = 5). The magnitude of the capacitance changes after the secretory phase for each stimulus is summarized in Fig. 6 *C*.

DISCUSSION

To begin the process of understanding the mechanisms underlying FcR-mediated phagocytosis, we examined time-resolved changes in membrane capacitance in single cells after stimulus binding and eventual phagosome formation. The temperature-dependent process appears to require the

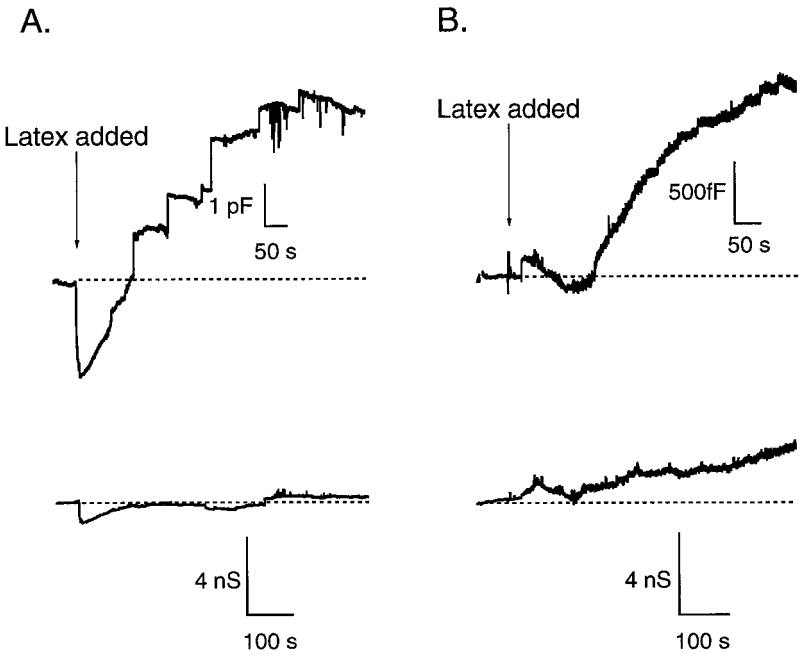

FIGURE 5 Exocytosis in two J774.1 cells, voltage clamped at −60 mV, as monitored by changes in membrane capacitance. Upper and lower traces in *A* and *B* show cell capacitance and series conductance, respectively. Cells were exposed to 3.2-μm beads in *A* and 0.8-μm beads in *B*. The upper traces show stepwise increases in capacitance occurring in the phagocytic cells after stimulation with latex particles at 37°C. Capacitance "flicker" as seen in *A*, or transient decreases in capacitance of relatively short duration, were absent from the exocytotic records as seen in *B*. Initial capacitances for cells in *A* and *B* were 22 and 8 pF, respectively.

actin cytoskeleton. Particle uptake is critically dependent upon the nature and size of the particle that is phagocytozed.

Phagocytosis of latex particles by HMDMs has previously been shown to be associated with increases in ion channel activity (Ince et al., 1988). Ince and co-workers, using the cell-attached mode of the patch clamp, were able to show, by video microscopy and the onset of enhanced ion channel activity, that phagocytosis of IgG-coated latex particles differed from phagocytosis of uncoated or albumin-coated particles by a shorter lag time between particle attachment and uptake (Ince et al., 1988). The whole-cell studies of Holevinsky and Nelson (1995) provided the first demonstration of the relationship between free radical release and the signaling events that are linked to particle engulfment in HMDMs. These studies demonstrated that whole-cell formation did not disrupt the cellular phagocytic machinery and, furthermore, that membrane depolarization and the generation of a calcium-dependent nonselective current followed an increase in superoxide production and phagocytic vacuole formation. Inasmuch as ion channel activation or changes in ionic conductance would produce artifactual changes in the capacitance measurements in the current studies, we used either pertussis toxin or the specific inhibitor of NADPH oxidase activation diphenylene iodonium (DPI), which was used previously (Holevinsky and Nelson, 1995), to block current activation. The onset of free radical release after particle uptake in our earlier studies (Holevinsky and Nelson, 1995) occurred with a lag time of ~140 s for 6-day-old HMDMs. Although we were unable to completely block the overlapping secretory response in the current studies, which would then allow us to accurately determine the onset of phagocytosis, the major decrement in membrane capacitance was seen well within the 140 s required to detect free radical release within the phagosome in our earlier studies.

Data in Fig. 2, in which capacitance changes would indicate that the cell ingested more than 300 latex beads 0.8 μm in size (assuming that individual particles were associated with the theoretically predicted value of 20 fF per particle), are consistent with the light microscope data in the Snyderman studies (Snyderman et al., 1977), in which single cells were capable of ingesting more than 200 latex particles. In Karrer's early studies of the phagocytic process in the lung (Karrer, 1960), which focused on the ultrastructure of the phagocytic vacuole, alveolar macrophages exposed to India ink were shown to be filled with vacuoles containing groups of particles. Micrographs demonstrated that large "flaps" or "ruffles" appeared to "trap large volumes of extracelluar material as the 'ruffles' backfold(ed) upon the cell." Therefore, assuming a membrane folding factor of 2.5, which is a conservative estimate from the studies of Karrer (1960), for each 0.8-μm latex particle one would expect a step size decrease in membrane capacitance of 50 fF. If each cell were to take up an average of 50 particles per cell, also a conservative estimate from the studies of Snyderman et al. (1977), this would predict a total average decrease of 2.5 pF per cell. This is very close to the average decrease in capacitance of 3.2 ± 1.3 pF for cells exposed to 0.8-μm beads.

From previous investigations it appears that phagocytic vacuole size varies in proportion to the size of the particle to be ingested, with no apparent threshold to the particle size necessary to initiate a phagocytic response (Griffin et al., 1975). The zipper model of phagocytosis first proposed by Griffin and colleagues (see review by Swanson and Baer, 1995) modeled the phagosome as conforming to the shape of the particle as a "close-fitting sleeve of plasma membrane." The complex was stabilized by particle interactions with surface receptors linked to the particle surface.

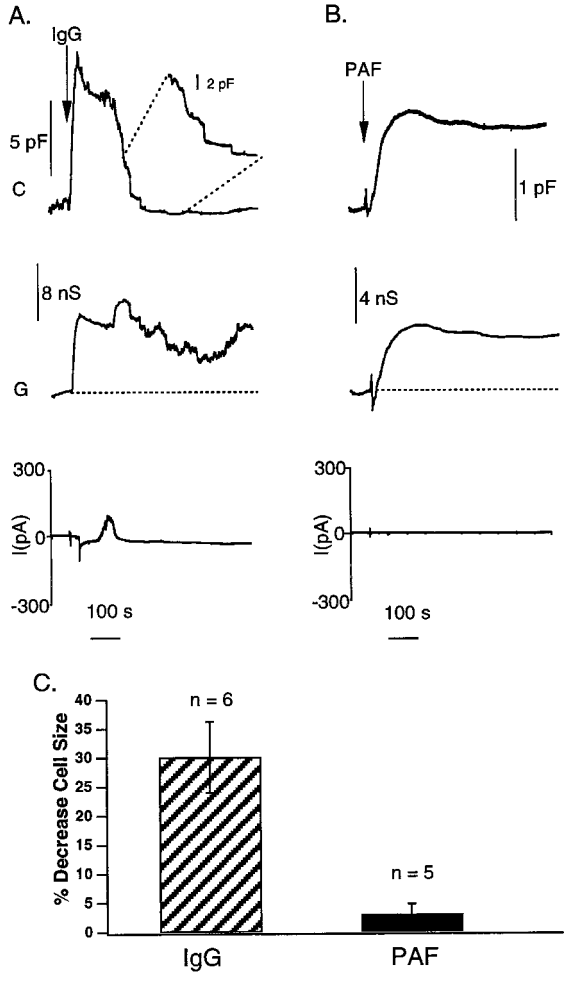

FIGURE 6 Comparison of changes in membrane capacitance after exposure of J774.1 cells to particulate and soluble stimuli. In these experiments, DPI (5 μM), a specific inhibitor of NADPH oxidase, was added to the bath solution 10 min before the exposure of the cells to either heat-aggregated human IgG (HAIGG) or PAF. Cells were voltage-clamped at 0 mV to minimize ion channel activity due to free-radical-generated current. Each panel consists of capacitance (*upper*), conductance (*middle*), and whole-cell (*lower*) current. (*A*) Continuous recording of membrane capacitance after exposure of a cell (28 pF) to 100 μg/ml IgG (indicated at the *arrow*) at 37°C. Note the biphasic nature of the response, consisting of a rapid secretory phase followed by a rapid reuptake phase that shows stepwise decreases that may correspond to the formation of individual phagocytic vesicles. (*B*) Recording of membrane capacitance changes after stimulation of a cell (25 pF) with PAF (20 ng/ml) added to the bath solution (indicated at the *arrow*). The experiment was performed at room temperature to inhibit phagocytosis. Note that unlike the response to particulate stimuli, PAF induced a monotonic increase in membrane capacitance that was not followed by rapid membrane reuptake. (*C*) Decrease in cell size after the peak secretory response, after the addition of either PAF or heat-aggregated IgG. Note that the peak of the exocytotic phase induced by HAIGG is an underestimate of the magnitude of the change, because it is likely that exocytosis and phagocytosis occur simultaneously.

Our data obtained using sized latex particles as the phagocytic stimulus would indicate that, although the size of the phagosome that is formed indeed scales with the size of the particle that is bound, the size of the phagosome is considerably larger than that which is theoretically predicted for a "tight sleeve." The experimentally observed event size distribution for each population of particles that were taken up by the phagocytes demonstrated that 1) there was a significant shift in the distribution of the step size with particle diameter and 2) there appeared to be significant membrane redundancy in the particle uptake mechanism. The latter observation is particularly evident with the smaller particles and may indicate that a step represents the endocytosis of a group of particles or "compound endocytosis." At small sizes, where the data seem to deviate significantly from the theoretically predicted mean value, the distribution may reflect two types of endocytotic processes occurring simultaneously, as has been proposed for the "off" response in nondegranulating mast cells (Fernandez et al., 1984). The "off" response, described by Fernandez and colleagues studying secretory mechanisms in mast cells, referred to step decreases in capacitance, which they occasionally observed using pipette solutions lacking GTP-γ-S. They attributed these step decreases to retrieval of excess membrane after a brief degranulation in response to whole-cell recording conditions.

The production of reactive oxygen molecules that accompanies Fc receptor ligation does not appear to be involved in phagosome formation. Pretreatment of cells with either pertussis toxin or DPI to inhibit NADPH oxidase activation did not inhibit phagosome formation, as monitored by changes in membrane capacitance. In previous studies (Holevinsky and Nelson, 1995), the lack of free-radical-induced current activation after exposure of the cells to immune complex provided evidence that toxin pretreatment inhibited the release of oxygen metabolites, but left open the question of whether phagosomes were formed in the presence of the inhibitors.

It has been speculated that both phagocytosis and NADPH oxidase are regulated at the level of the small GTP-binding protein Rac activation (Knaus et al., 1991; Bokoch, 1995). Although important in the signal transduction cascade, carrying surface binding events to nuclear transcriptional events, small GTP-binding proteins do not appear to be important in the process of phagosome formation. In our experiments, phagocytosis and exocytosis occur in the absence of exogenous guanine or adenosine nucleotides added to the pipette solution, which dilutes cellular contents in the whole-cell patch-clamp configuration.

Macrophages stimulated with either soluble or particulate ligands undergo a secretory phase, the onset of which is much more rapid in the case of the particulate ligand. The magnitude of the secretory response, however, does not appear to depend upon the secretory stimulus. Capacitance measurements of exocytosis or degranulation in cells of the immune system have provided unique insight into the signal transduction mechanisms in excitation-secretion coupling. Secretion in mast cells and neutrophils, unlike in their excitable cell counterparts, does not require an influx of extracellular Ca^{2+} through a plasma membrane conductance, but rather seems to be coupled to intracellular levels of guanine nucleotides and Ca^{2+} released from internal

stores (Fernandez et al., 1984; Lindau and Fernandez, 1986; Lindau, 1988; Neher, 1988, 1991; Nuesse and Lindau, 1988; Matthews et al., 1989). The steps leading to granule fusion in mast cells as well as neutrophils are controlled by a guanine nucleotide-binding protein. Although changes in intracellular Ca^{2+} (Ca_i) appear to be involved in the regulation or rate of degranulation (Neher, 1988; Nuesse and Lindau, 1988), elevation of Ca_i is not a sufficient stimulus to promote secretion on its own. Our data from macrophages indicate that degranulation is not tightly linked to levels of guanine nucleotides. Secretion in response to both stimuli occurs in the absence of the addition of guanine nucleotides to the pipette solution. Membrane retrieval that was observed in mast cells after a secretory response (Fernandez et al., 1984) was not observed in response to soluble stimuli in macrophages. Thus the endocytic response after Fc receptor ligation with particulate stimuli can be attributed primarily to phagosomal vacuole formation. Furthermore, rapid membrane retrieval in macrophages does not appear to be tightly linked to the secretory response per se, as is the case for synaptic vesicle recycling in synaptic terminals (von Gersdorff and Matthews, 1994), and may be more closely coupled to the receptor type that initiates the secretory response.

The authors thank Drs. R. J. Bookman, A. P. Fox, and F. S. Cohen for many helpful discussions and advice during the course of these studies.

This work was supported by grants from the National Institutes of Health (RO1 GM36823 and RO1 GM54266) and a grant from the Cystic Fibrosis Foundation.

REFERENCES

Artalejo, C. R., M. E. Adams, and A. P. Fox. 1994. Three types of Ca^{2+} channel trigger secretion with different efficacies in chromaffin cells. *Nature.* 367:72–76.

Artalejo, C. R., A. Elhamdani, and H. C. Palfrey. 1996. Calmodulin is the divalent cation receptor for rapid endocytosis, but not exocytosis, in adrenal chromaffin cells. *Neuron.* 16:195–205.

Artalejo, C. R., J. R. Henley, M. A. McNiven, and H. C. Palfrey. 1995. Rapid endocytosis coupled to exocytosis in adrenal chromaffin cells involves Ca^{2+}, GTP, and dynamin but not clathrin. *Proc. Natl. Acad. Sci. USA.* 92:8328–8332.

Bokoch, G. M. 1995. Regulation of the phagocyte respiratory burst by small GTP-binding proteins. *Trends Cell Biol.* 5:109–113.

Breckenridge, L. J., and W. Almers. 1987a. Currents through the fusion pore that forms during exocytosis. *Nature.* 328:814–817.

Breckenridge, L. J., and W. Almers. 1987b. Final steps in exocytosis observed in a cell with giant secretory granules. *Proc. Natl. Acad. Sci. USA.* 84:1945–1949.

Fernandez, J. M., E. Neher, and B. D. Gomperts. 1984. Capacitance measurements reveal stepwise fusion events in degranulating mast cells. *Nature.* 312:453–455.

Fidler, N. H., and J. M. Fernandez. 1989. Phase tracking: an improved phase detection technique for cell membrane capacitance measurements. *Biophys. J.* 56:1153–1162.

Fidler-Lim, N. F., M. C. Nowycky, and R. J. Bookman. 1990. Direct measurement of exocytosis and calcium currents in single vertebrate nerve terminals. *Nature.* 344:449–451.

Griffin, F. M., J. A. Griffin, J. E. Leider, and S. C. Silverstein. 1975. Studies on the mechanism of phagocytosis. I. Requirements for circumferential attachment of particle-bound ligands to specific receptors on the macrophage plasma membrane. *J. Exp. Med.* 142:1263–1282.

Hamill, O. P., A. Marty, E. Neher, and B. Sakmann. 1981. Improved patch-clamp techniques for high resolution current recording from cells and cell-free membrane patches. *Pflügers Arch. Eur. J. Physiol.* 391: 85–100.

Henson, P. M., J. E. Henson, C. Fittschen, G. Kimani, D. L. Bratton, and D. W. H. Riches. 1988. Phagocytic cells: degranulation and secretion. *In* Inflammation: Basic Principles and Clinical Correlates. J. I. Gallin, J. M. Goldstein, and R. Snyderman, editors. Raven Press, New York. 363–390.

Holevinsky, K. O., and D. J. Nelson. 1995. Simultaneous detection of free radical release and membrane current during phagocytosis. *J. Biol. Chem.* 270:8328–8336.

Horrigan, F. T., and R. J. Bookman. 1994. Releasable pools and the kinetics of exocytosis in adrenal chromaffin cells. *Neuron.* 13: 1119–1129.

Ince, C., J. M. C. C. Coremans, D. L. Ypey, P. C. J. Leijh, A. A. Verveen, and R. v. Furth. 1988. Phagocytosis by human macrophages is accompanied by changes in ionic channel currents. *J. Cell Biol.* 106: 1873–1878.

Joshi, C., and J. M. Fernandez. 1988. Capacitance measurements: an analysis of the phase detector technique used to study exocytosis and endocytosis. *Biophys. J.* 53:885–892.

Kaplan, G., and B. Morland. 1978. Properties of a murine monocytic tumor cell line J-774 in vitro. *Exp. Cell Res.* 115:53–61.

Karrer, H. E. 1960. Electron microscopic study of the phagocytosis process in lung. *J. Biophys. Biochem. Cytol.* 7:357–391.

Katnik, C., and D. J. Nelson. 1993. Platelet activating factor-induced increase in cytosolic calcium and transmembrane current in human macrophages. *J. Membr. Biol.* 134:213–224.

Knaus, U. G., P. G. Heyworth, T. Evans, J. T. Curnutte, and G. M. Bokoch. 1991. Regulation of phagocyte oxygen radical production by the GTP-binding protein Rac 2. *Science.* 254:1512–1515.

Kubo, Y., T. J. Baldwin, Y. N. Jan, and L. Y. Jan. 1993. Primary structure and functional expression of a mouse inward rectifier potassium channel. *Nature.* 362:127–133.

Lindau, M., and J. M. Fernandez. 1986. IgE-mediated degranulation of mast cells does not require opening of ion channels. *Nature.* 319: 150–153.

Lindau, M., and E. Neher. 1988. Patch-clamp techniques for time-resolved capacitance measurements in single cells. *Pflügers Arch.* 411:137–146.

Matthews, G., E. Neher, and R. Penner. 1989. Second messenger-activated calcium influx in rat peritoneal mast cells. *J. Physiol. (Lond.).* 418: 105–130.

Morland, B., and G. Kaplan. 1978. Properties of a murine monocytic tumor cell line J-774 in vitro. II. Enzyme activities. *Exp. Cell Res.* 115:63–72.

Neher, E. 1988. The influence of intracellular calcium concentration on degranulation of dialysed mast cells from rat peritoneum. *J. Physiol. (Lond.).* 395:193–214.

Neher, E. 1991. Ion influx as a transduction signal in mast cells. *Int. Arch. Allergy Appl. Immunol.* 94:47–50.

Neher, E., and A. Marty. 1982. Discrete changes of cell membrane capacitance observed under conditions of enhanced secretion in bovine adrenal chromaffin cells. *Proc. Natl. Acad. Sci. USA.* 79:6712–6716.

Nelson, D. J., E. R. Jacobs, J. M. Tang, J. M. Zeller, and R. C. Bone. 1985. Immunoglobulin G-induced single ionic channels in human alveolar macrophage membranes. *J. Clin. Invest.* 76:500–507.

Nelson, D. J., B. Jow, and F. Jow. 1990. Whole-cell currents in macrophages. I. Human monocyte-derived macrophages. *J. Membr. Biol.* 117:29–44.

Nuesse, O., and M. Lindau. 1988. The dynamics of exocytosis in human neutrophils. *J. Cell Biol.* 107:2117–2123.

Odin, J. A., J. C. Edberg, C. J. Painter, R. P. Kimberly, and J. C. Unkeless. 1991. Regulation of phagocytosis and $[Ca^{2+}]_i$ flux by distinct regions of an Fc receptor. *Science.* 254:1785–1788.

Odin, J. A., C. J. Painter, and J. C. Unkeless. 1990. Fcγ receptors: a diverse and multifunctional gene family. *In* Cellular and Molecular Mechanisms of Inflammation. C. G. Cochrane and J. Gimbrone, editors. Academic Press, San Diego. 1–34.

Parsons, T., D. Lenzi, W. Almers, and W. M. Roberts. 1994. Calcium-triggered exocytosis and endocytosis in an isolated presynaptic cell: capacitance measurements in saccular hair cells. *Neuron.* 33:875–883.

Ryan, T. C., G. J. Weil, P. E. Newburger, R. Haugland, and E. R. Simons. 1990. Measurement of superoxide release in the phagovacuoles of immune complex-stimulated human neutrophils. *J. Immunol. Methods.* 130:223–233.

Schweizer, F. E., T. Schäfer, C. Tapparelli, M. Grob, U. O. Karli, R. Heumann, H. Thoenen, R. J. Bookman, and M. M. Burger. 1989. Inhibition of exocytosis by intracellularly applied antibodies against a chromaffin granule-binding protein. *Nature.* 339:709–712.

Smith, C. B., and W. J. Betz. 1996. Simultaneous independent measurement of endocytosis and exocytosis. *Nature.* 380:531–534.

Snyderman, R., M. C. Pike, D. G. Fischer, and H. S. Koren. 1977. Biologic and biochemical activities of continuous macrophage cell lines P388D1 and J774.1. *J. Immunol.* 119:2060–2066.

Solsona, C., B. Innocenti, and J. M. Fernandez. 1998. Regulation of exocytotic fusion by cell inflation. *Biophys. J.* 74:1061–1073.

Suzuki, T. 1991. Signal transduction mechanisms through Fcγ receptors on the mouse macrophage surface. *FASEB J.* 5:187–193.

Swanson, J. A., and S. C. Baer. 1995. Phagocytosis by zippers and triggers. *Trends in Cell Biol.* 5:89–93.

Thomas, P., A. Suprenant, and W. Almers. 1990. Cytosolic Ca^{2+}, exocytosis, and endocytosis in single melanotrophs of the rat pituitary. *Neuron.* 5:723–733.

von Gersdorff, H., and G. Matthews. 1994. Dynamics of synaptic vesicle fusion and membrane retrieval in synaptic terminals. *Nature.* 367: 735–739.

Voronov, I., J. P. Santerre, A. Hinek, J. W. Callahan, J. Sandhu, and E. L. Boynton. 1998. Macrophage phagocytosis of polyethylene particulate in vitro. *J. Biomed. Mater. Res.* 39:40–51.

Wright, S. D., and S. C. Silverstein. 1982. Tumor-promoting phorbol esters stimulate C3b and C3b′ receptor-mediated phagocytosis in cultured human monocytes. *J. Exp. Med.* 156:1149–1164.

Zimmerberg, J., M. Curran, F. S. Cohen, and M. Brodwick. 1987. Simultaneous electrical and optical measurements show that membrane fusion precedes secretory granule swelling during exocytosis of beige mouse mast cells. *Proc. Natl. Acad. Sci. USA.* 841:1585–1589.